JNeurosci
THE JOURNAL OF NEUROSCIENCE

Research Articles: Neurobiology of Disease

Inhibition of p25/Cdk5 attenuates tauopathy in mouse and iPSC models of frontotemporal dementia

Jinsoo Seo[1,2], Oleg Kritskiy[1], L. Ashley Watson[1,2], Scarlett J. Barker[1,2], Dilip Dey[1], Waseem K Raja[1,2], Yuan-Ta Lin[1,2], Tak Ko[1], Sukhee Cho[1], Jay Penney[1,2], M. Catarina Silva[3], Steven D. Sheridan[3], Diane Lucente[4], James F. Gusella[4], Bradford C. Dickerson[5], Stephen J. Haggarty[3] and Li-Huei Tsai[3]

[1]*Picower Institute for Learning and Memory, Massachusetts Institute of Technology, Cambridge, MA 02139, USA.*

[2]*Department of Brain and Cognitive Sciences, Massachusetts Institute of Technology, Cambridge, MA 02139, USA.*

[3]*Center for Genomic Medicine, Chemical Neurobiology Laboratory, Departments of Neurology & Psychiatry, Massachusetts General Hospital and Harvard Medical School, Boston, MA 02114, USA.*

[4]*Molecular Neurogenetics Unit, Center for Genomic Medicine, Massachusetts General Hospital and Harvard Medical School, Boston, MA 02114, USA.*

[5]*MGH Frontotemporal Disorders Unit, Gerontology Research Unit, and Alzheimer's Disease Research Center, Department of Neurology, Massachusetts General Hospital and Harvard Medical School, Charlestown, Massachusetts 02129, USA.*

[6]*Broad Institute of Harvard and Massachusetts Institute of Technology, Cambridge, MA 02142, USA.*

DOI: 10.1523/JNEUROSCI.0621-17.2017

Received: 6 March 2017

Revised: 15 August 2017

Accepted: 4 September 2017

Published: 14 September 2017

Author contributions: J.S., O.K., S.C., and L.-H.T. designed research; J.S., O.K., S.J.B., D.D., W.K.R., Y.-T.L., S.C., and J.P. performed research; J.S., O.K., S.J.B., S.C., and J.P. analyzed data; J.S., A.W., and L.-H.T. wrote the paper; A.W., W.K.R., Y.-T.L., T.K., C.S., S.D.S., D.L., J.G., B.C.D., and S.J.H. contributed unpublished reagents/analytic tools.

Conflict of Interest: The authors declare no competing financial interests.

The authors would like to thank all members of Tsai lab for advice and discussion. Ting Fu is thanked for technical assistance with iPSC reprogramming. This work was supported by the National Institutes of Health (NIH) grant R37NS051874 and the Robert A. and Renee E. Belfer Family Foundation and Belfer Neurodegeneration Consortium to L.-H.T. NIH/NINDS grant R21NS085487 to S.J.H. and B.C.D., Association for Frontotemporal Degeneration to M.C.S., Tau Consortium to S.J.H.

Correspondence should be addressed to Li-Huei Tsai (lhtsai@mit.edu)

Cite as: J. Neurosci ; 10.1523/JNEUROSCI.0621-17.2017

Inhibition of p25/Cdk5 attenuates tauopathy in mouse and iPSC models of frontotemporal dementia

Jinsoo Seo[1,2,7], Oleg Kritskiy[1,7], L. Ashley Watson[1,2], Scarlett J. Barker[1,2], Dilip Dey[1], Waseem K Raja[1,2], Yuan-Ta Lin[1,2], Tak Ko[1], Sukhee Cho[1], Jay Penney[1,2], M. Catarina Silva[3], Steven D. Sheridan[3], Diane Lucente[4], James F. Gusella[4], Bradford C. Dickerson[5], Stephen J. Haggarty[3] and Li-Huei Tsai[1,2,6].

[1] Picower Institute for Learning and Memory, Massachusetts Institute of Technology, Cambridge, MA 02139, USA.

[2] Department of Brain and Cognitive Sciences, Massachusetts Institute of Technology, Cambridge, MA 02139, USA.

[3] Center for Genomic Medicine, Chemical Neurobiology Laboratory, Departments of Neurology & Psychiatry, Massachusetts General Hospital and Harvard Medical School, Boston, MA 02114, USA.

[4] Molecular Neurogenetics Unit, Center for Genomic Medicine, Massachusetts General Hospital and Harvard Medical School, Boston, MA 02114, USA.

[5] MGH Frontotemporal Disorders Unit, Gerontology Research Unit, and Alzheimer's Disease Research Center, Department of Neurology, Massachusetts General Hospital and Harvard Medical School, Charlestown, Massachusetts 02129, USA.

[6] Broad Institute of Harvard and Massachusetts Institute of Technology, Cambridge, MA 02142, USA.

[7] These authors contributed equally to this work.

Correspondence should be addressed to Li-Huei Tsai (lhtsai@mit.edu)

Abbreviated title : p25 inhibition attenuates tauopathy

33 pages, 4 figures, abstract - 214 words, introduction – 805 words, discussion – 845 words

Conflict of interest: The authors declare no competing financial interests.

Acknowledgements

The authors would like to thank all members of Tsai lab for advice and discussion. Ting Fu is thanked for technical assistance with iPSC reprogramming. This work was supported by the National Institutes of Health (NIH) grant R37NS051874 and the Robert A. and Renee E. Belfer Family Foundation and Belfer Neurodegeneration Consortium to L.-H.T. NIH/NINDS grant R21NS085487 to S.J.H. and B.C.D., Association for Frontotemporal Degeneration to M.C.S., Tau Consortium to S.J.H.

Abstract

Increased p25, a proteolytic fragment of the regulatory subunit p35, is known to induce aberrant activity of cyclin-dependent kinase 5 (Cdk5), which is associated with neurodegenerative disorders including Alzheimer's disease (AD). Previously, we showed that replacing endogenous p35 with the non-cleavable mutant p35 (Δp35) attenuated amyloidosis and improved cognitive function in a familial AD mouse model. Here, to address the role of p25/Cdk5 in tauopathy, we generated double transgenic mice by crossing mice overexpressing mutant human tau (P301S) with Δp35KI mice. We observed significant reduction of phosphorylated tau and its seeding activity in the brain of double transgenic mice compared to the P301S mice. Furthermore, synaptic loss and impaired LTP at hippocampal CA3 region of P301S mice were attenuated by blocking p25 generation. To further validate the role of p25/Cdk5 in tauopathy, we utilized frontotemporal dementia (FTD) patient-derived induced pluripotent stem cells (iPSCs) carrying the Tau P301L mutation and generated P301L:Δp35KI isogenic iPSC lines using CRISPR/Cas9 genome editing. We created cerebral organoids from the isogenic iPSCs and found that blockade of p25 generation reduced levels of phosphorylated tau and increased expression of synaptophysin. Together, these data demonstrate a crucial role for p25/Cdk5 in mediating tau-associated pathology and suggest that inhibition of this kinase can remedy neurodegenerative processes in the presence of pathogenic tau mutation.

Significance statement

Accumulation of p25 results in aberrant Cdk5 activation and induction of numerous pathological phenotypes such as neuroinflammation, synaptic loss, Aβ accumulation and tau hyperphosphorylation. However, it was not clear whether p25/Cdk5 activity is necessary for the progression of these pathological changes. We recently developed the Δp35KI transgenic mouse that is deficient in p25 generation and Cdk5 hyperactivation. In this study, we utilized this mouse model to elucidate the role of p25/Cdk5 in FTD mutant tau-mediated pathology. We also employed a FTD patient-derived iPSCs carrying the Tau P301L mutation and generated isogenic lines in which p35 is replaced with non-cleavable mutant Δp35. Our data suggest that p25/Cdk5 plays an important role in tauopathy in both mouse and human model systems.

Introduction

Tau is a microtubule-binding protein, which stabilizes and promotes assembly of microtubules. Hyperphosphorylation, insolubilization and accumulation of tau is observed in various neurodegenerative diseases including Alzheimer's disease (AD) and frontotemporal dementia (FTD). Tau hyperphosphorylation can lead to a conformational change of the protein that triggers its dissociation from microtubules and reduced microtubule integrity. The breakdown of this tubular system disrupts intracellular organelle transport, such as the movement of mitochondria or other cargos to peripheral regions, which eventually results in the degeneration of axons (Mazanetz and Fischer, 2007; Kolarova et al., 2012; Kondadi et al., 2014). Abnormal phosphorylation of tau also leads to its mislocalization to dendritic spines, resulting in synaptotoxicity through the abnormal recruitment of tau-binding proteins such as a Fyn kinase into the synapse (Ittner et al., 2010).

Cyclin-dependent kinase 5 (Cdk5) is a serine/threonine kinase whose activity is necessary for neuronal migration, synapse development and synaptic plasticity. Cdk5 is not catalytically active unless it is associated with a regulatory activator, such as p35. The abundance of p35 is regulated by two alternate pathways consisting of the rapid proteasomal degradation of p35, or the direct truncation of p35 to a soluble 25 kDa form (p25) by calpain, a Ca^{2+}-dependent cysteine protease. Whereas the former is common under physiological conditions, the latter is primarily associated with the function of Cdk5 under pathological conditions

115 (Patrick et al., 1999; Ahlijanian et al., 2000; Kusakawa et al., 2000; Lee et al., 2000;
116 Nath et al., 2000).
117
118 To date, a large body of literature supports the role of Cdk5 in numerous
119 pathological phenotypes in neurodegenerative disorders, including AD. For
120 example, work in various neurodegenerative disease model systems or animal
121 models of AD showed that pharmacological inhibition or targeted knockdown of
122 Cdk5 relieved neurotoxicity and tau pathology (Piedrahita et al., 2010; Zhang et al.,
123 2013a; Miller et al., 2015). The ability of Cdk5 to phosphorylate tau (pTau) was
124 shown to be enhanced in the presence of p25 compared to p35 (Van den Haute et al.,
125 2001; Hashiguchi et al., 2002; Noble et al., 2003). Consistent with these findings,
126 several p25-overexpressing transgenic mouse models exhibit tau
127 hyperphosphorylation and aggregation (Cruz et al., 2003; Noble et al., 2003).
128 Altogether, these studies show that p25/Cdk5 induce tauopathy.
129 A recent study reported that p25 expression is increased in the brain of JNPL3 mice
130 carrying a human mutant transgene harboring a P301L mutation. And inhibition of
131 calpain was reduced p25 levels and attenuated tauopathy in these mice (Rao et al.,
132 2014). It suggests that in addition to p25/Cdk5 inducing tauopathy, p25 production
133 can itself be regulated by pathogenic tau. The novel question that we have not yet
134 answered is whether or not p25 generation is a key factor in developing pathogenic
135 tau mutation-induced pathology. Furthermore, it remains unclear if p25/Cdk5
136 mediates tauopathy in patient-derived cell models. Recently, we developed the
137 knock-in mouse (Δp35KI) incapable of generating p25 (Seo et al., 2014). In this

work, we thoroughly characterized the Δp35KI mouse through biochemical, electrical and behavioral assays. We did not observe any difference in Cdk5 activity between WT and Δp35KI mice, which is consistent with the fact that expression of p25 under basal conditions is low. These mice exhibit impaired long-term depression in hippocampal Schaffer collateral-CA1 synapses and a deficit in memory extinction suggesting the role of activity-induced p25 in memory process. However, overall they display normal brain development, synapse density, locomotion and learning behavior. And no obvious pathological phenotype was observed in Δp35KI mice. In the current study, we utilize this mouse line to inhibit p25 generation in a mouse model of FTD.

Previous studies using isogenic human induced pluripotent stem cells (iPSCs) derived from AD, FTD or Down syndrome (DS) individuals have shown that these cells display a number of readily observable disease phenotypes (Israel et al., 2012; Mou et al., 2012; Fong et al., 2013; Zhang et al., 2013b; Silva et al., 2016). The iPSC model system provides a critically needed means by which to conduct mechanistic studies in living human cells. Moreover, the advent of the clustered regularly interspaced short palindromic repeats (CRISPR) system using the Cas9 nuclease to induce guided DNA breaks provides a major advance in our ability to manipulate the human genome (Komor et al., 2017). Lastly, three-dimensional (3D) human neural culture systems, also known as cerebral organoids, have been recently developed to better recapitulate some specific features of the human brain such as architectural complexity and cortical layer formation. We recently found that cerebral organoids

161 derived from familial AD patient iPSCs endogenously develop Aβ and tau
162 aggregation, which has not been observed in conventional two-dimensional (2D)
163 culture systems (Raja et al., 2016). In the current study, we generated Δp35KI iPSCs
164 from fibroblasts of a FTD patient by reprogramming along with genome editing
165 techniques, which enabled us to address the role of p25/Cdk5 in a human tauopathy
166 model.
167
168
169
170
171
172
173
174
175
176
177
178
179
180
181
182
183

Materials & Methods

Animals

All animal experiments were performed with approval from the MIT Committee on Animal Care (CAC). P301S Tg mice (PS19) (Yoshiyama et al., 2007) were obtained from the Jackson Laboratory (https://www.jax.org/strain/008169, Bar Harbor, ME, USA) and crossed to the Δp35KI mouse to generate P301S;Δp35KI mice. 4-month-old littermates were used for all the experiments, if not other indicated. Male mice were used for electrophysiology experiments, and Female mice were used for all biochemistry experiments.

Immunoblot Analysis

Hippocampal or cortical tissues were homogenized in RIPA buffer (50 mM Tris, pH 8.0, 150 mM NaCl, 1% NP-40, 0.5% sodium deoxycholate, 0.1% SDS) containing protease and phosphatase inhibitors. For organoids, 3~4 organoids were pooled, homogenized and sonicated in RIPA buffer. Lysates were incubated on ice for 15 min and spun at 12,000 rpm for 15 min. Then, supernatants were transferred to new tubes and analyzed for protein concentration (Bio-Rad Protein Assay). SDS buffer was added to equal amounts of protein and subjected to SDS-PAGE and immunoblotting analysis.

Antibodies

p35 (Dr. Li-Huei Tsai's lab), Cdk5, HA, GAPDH (Santa Cruz Biotechnology), pTau T181, pTau S202 (Cell Signaling Technology), Synaptophysin (Sigma-Aldrich), NeuN (Synaptic Systems), Tau5 (Thermo Fisher Scientific)

IP-linked kinase assay

Hippocampal lysates were incubated with a anti-Cdk5 antibody for overnight at 4°C and the immunocomplex was subjected to a Cdk5 kinase assay as described previously (Seo et al., 2014).

Immunohistochemistry

Mice were transcardially perfused with 4% paraformaldehyde in PBS under anesthesia (2:1 of ketamine/xylazine), and the brains were sectioned at 40 μm thickness with a Leica VT1000S vibratome (Leica). Slices were permeabilized with blocking solution containing 0.1% Triton X-100, 1 M glycine, 10% donkey serum and 2% BSA in PBS for 1 hr at room temperature, and incubated at 4°C for overnight with blocking solution containing primary antibody. Slices were then incubated at room temperature for 1 hr with fluorescently conjugated secondary antibodies (Molecular Probes), and nuclei were stained with Hoechst 33342 (Invitrogen).

Microscopy

All images were captured using a Zeiss LSM 880 confocal microscope and the ZEN software, and analyzed using the ImageJ software (National Institutes of Health, https://imagej.nih.gov/ij/, RRID: SCR_003070).

Tau seeding activity assay

Brains were homogenized in 1XTBS supplemented with protease inhibitors using a probe sonicator (30% power; 15 pulses). After sonication, the lysates were centrifuged at 16,000 x g for 15 min to eliminate large, insoluble material. The supernatant was stored at -80 °C and used for all future experiments. Protein concentration was determined using a Bio-Rad Protein Assay Kit. FRET biosensor cell lines described previously (Holmes et al., 2014) were provided by Marc I. Diamond. Cells were grown in Dulbecco's modified Eagle's medium (Gibco) augmented with 10% fetal bovine serum and 1X penicillin/streptomycin and maintained at 37 °C and 5% CO2 in a humidified incubator. For the assay, cells were plated in a 96-well plate at a density of 40,000 cells/well. Sixteen hours later, at 50% confluence, brain homogenate samples were transduced into cells using 1 uL Lipofectamine/well. After a 48-hour incubation at 37 °C, cells were harvested with 0.25% trypsin and fixed in 4% paraformaldehyde (Electron Microscopy Services) for 15 min, and then resuspended in PBS. An LSR II HST-2 flow cytometer was used to measure the FRET signal within each cell. FRET quantification was accomplished using FlowJo v10 software (Treestar Inc.). Integrated FRET density was derived by multiplying the percent of FRET-positive cells in each sample by the median FRET intensity of those cells.

Electrophysiology

Hippocampal slices (transverse, 400 μm-thick) were prepared in ice-cold dissection buffer (in mM: 211 sucrose, 3.3 KCl, 1.3 NaH_2PO_4, 0.5 $CaCl_2$, 10 $MgCl_2$, 26 $NaHCO_3$ and 11 glucose) using a Leica VT1000S vibratome (Leica). Slices were then moved to the submerged chamber with 95% O_2/5% CO_2-saturated artificial cerebrospinal fluid (ACSF) consisting of (mM) 124 NaCl, 3.3 KCl, 1.3 NaH_2PO_4, 2.5 $CaCl_2$, 1.5 $MgCl_2$, 26 $NaHCO_3$ and 11 glucose at 30 °C for at least 1 hr before the recording. Extracellular recording at mossy fiber-CA3 synapses were performed as previously described (Siegert et al., 2015). In brief, a tungsten bipolar electrode was placed in the dentate granule cell layer to stimulate mossy fibers, and extracellular recordings were made in the stratum lucidum of CA3 using a glass microelectrode filled with ACSF (resistance of 2-3 MΩ). LTP was induced by three trains of high frequency stimulation (100 Hz for 1 sec) with 10 sec intervals after observation of stable baseline. To verify mossy fiber inputs, 1 μM (2S,2′R,3′R)-2-(2′,3′ dicarboxycyclopropyl)glycine (DCG-IV; Tocris Bioscience), a group II metabotropic glutamate receptor agonist that selectively blocks mossy fiber responses, was applied at the end of each recording. The amplitude of fEPSPs was measured to quantify the strength of synaptic transmission. A MultiClamp 700B amplifier and a Digidata 1440A A-D converter (Axon Instruments) were used for data acquisition and data were analyzed with pClamp10 (Axon Instruments).

iPSC cultures

FTD patient (Tau P301L carrier) and related healthy individual dermal fibroblasts were generated from a skin biopsy from subjects within the MGH Frontotemporal

Dementia Clinic as part of the MGH Neurodegeneration Repository. Approval for human subjects work was obtained under a Partners/MGH-approved IRB Protocol (#2010P001611/MGH). iPSCs (Tau-P301L MGH-2046 and non-mutant control MGH-2069) were generated using a synthetic modified mRNA-based reprogramming method (StemGent mRNA Modified Reprogramming Kit). These iPSC lines have been fully characterized and presence of the P301L mutation in *MAPT* was confirmed by sequencing (*Silva, Watson, Tsai, Haggarty et al., Manuscript in preparation*). iPSCs were cultured on irradiated mouse embryonic fibroblasts (MEFs, MTI-GlobalStem) in DMEM/F12, HEPES media (Gibco) supplemented with 20% knockout serum replacement (KSR) (Gibco), 1X non-essential amino acids (NEAA), 1X GlutaMAX, (Life Technologies) beta-fibroblast growth factor (FGF2, PeproTech) and 0.1 mM 2-mercaptoethanol (Sigma-Aldrich) and maintained at 37 °C and 5% CO2 in a humidified incubator.

Generation of Δp35KI isogenic lines

a. Preparation of the CRISPR/Cas9-p35-sgRNA plasmid

A sgRNA for targeting *CDK5R1* gene (GGGGCTGGGCGAATGTGGAC, reverse) was designed by http://crispr.mit.edu. And both sgRNA and repair template (ssODNs: TGAGGGGCTTTCTTGACTGAGGAGGAGCCCCCGGTCTGGGAACCCGAGAGCTGGCTGGCC GGGGGTGCAGGCGGCTGGGCCGGTGGGGGCTGGAGGCACGACAGCGACTTCTTCAGGTTC TCATTGTTGAGGTGCGTGATGTTGTTCTGGTAGCTGCTGTTGGGCTGCACCTTCTTGGAG TTCTTCTTCTTGG) were synthesized by IDT (Integrated DNA Technologies). The CRISPR/Cas9 plasmid (pSpCas9-2A-GFP, PX458) was purchased from Addgene and

297 the p35-sgRNA was cloned into the plasmid as described previously (Ran et al.,
298 2013).
299
300 *b. Electroporation*
301 iPSCs on MEFs plates were dissociated with Accutase (Thermo Fisher Scientific) and
302 collected to a 15-ml falcon tube. Cells were washed with hES media once and then
303 resuspended with hES media to count the number of cells. 5 million cells were
304 transferred to a new tube and media was removed. Then, the CRISPR/Cas9-p35-
305 sgRNA and ssODNs were added to cells, mixed and transferred to a cuvette. The
306 Nucleofector™ (Amaxa) and the Human Stem Cell Nucleofector Kit 1 (Lonza) were
307 used for the electroporation and the cells were resuspended in hES media with 10
308 μM ROCK inhibitor and transferred to a new MEFs plates.
309
310 *c. Fluorescence-activated cell sorting (FACS)*
311 Two days after the electroporation, cells were dissociated with accutase and
312 transferred to a 15-ml falcon tube. Cells were washed with hES media once,
313 resuspended with DPBS and filtered using falcon polystyrene test tube (#2235).
314 Filtered cells were collected and sorted by a Becton Dickinson Aria II based on GFP
315 signal. Sorted cells were then collected in hES media with 1X
316 penicillin/streptomycin and 10 μM Rho-associated protein kinase (ROCK) inhibitor
317 (Y-27632, Millipore) and plated at a density of 80,000 cells/well.
318
319 *d. Colony inspection*

Once colonies formed, single colonies were transferred to each well of 12-well MEFs plates. After second transfer, cells in the original plates were dissociated and genomic DNAs were extracted as previously described (Ran et al., 2013). PCR was performed with the primer set to target the CDK5R1 gene (p35F-CTGTCCCTGTCTCCCAGCTA, p35R-GGCAGAGAAACTCACCCAGG) and the PCR product was submitted to Genewiz for the sequencing.

Organoid culture

Organoids were created from iPSCs carrying the Tau P301L mutation, the Δp35KI isogenic or healthy control lines using the protocol described previously (Raja et al., 2016). In brief, embryoid bodies (EBs) were formed by loading 12,000 iPSCs per well into 96-well plates pre-coated with Pluronic acid (1%, F-127, Sigma-Aldrich). EBs were maintained in the Media 1 consists of Glasgow-MEM supplement with 20 % KSR, 1X sodium pyruvate, 1X NEAA, 0.1 mM 2-mercaptoethanol, 20 μM ROCK inhibitor (Y-27632, Millipore), 5 μM TGFβ-inhibitor (SB431532, Tocris Biosciences), 3 μM Wnt-inhibitor (IWRe1, Tocris Biosciences) for 20 days. Dorsomorphin, a BMP inhibitor (2 μM Tocris Biosciences) was added for the first three days. Organoids were then transferred to non-adherent petri-dishes and cultured in the Media 2 consisted of DMEM/F12 supplemented with 1X Chemically Defined Lipid Concentrate and 1X N2-supplement with 40% O_2/5% CO_2 to promote neuroepithelial formation. From day 35, 5 μM heparin (Sigma-Aldrich), 10% FBS and 1% matrigel (Life Sciences) were added to the medium.

343 *Experimental Design and Statistical analysis*

344 Data are mean ± S.E.M. and were analyzed by Prism 6 software (GraphPad).
345 Student's *t* test was used to compare the means of two groups. One-way ANOVA
346 followed by Tukey's post hoc analysis was used for multiple comparison. p <0.05
347 was considered significant.

348

349

350

351

352

353

354

355

356

357

358

359

360

361

362

363

364

365

Results

Abnormal p25 expression induces hyperactivation of Cdk5 in the brain of P301S mice.

To first test whether p25 levels are affected by pathogenic tau, we used a C-terminal specific p35 antibody to detect both p35 and p25 species in the brain of P301S transgenic mice. Using hippocampal lysates from 4-month-old mice, we observed a two-fold increase in p25/p35 ratio in P301S mice compared to that of WT (Figure 1A, B, p=0.030). To measure Cdk5 activity in these samples, we immunoprecipitated Cdk5 then performed a kinase assay using radiolabeled ATP and histone H1 protein, as a substrate of Cdk5. We found that basal Cdk5 activity in P301S mouse hippocampus is significantly increased compared to WT (Figure 1C, p=0.0009 by ANOVA). To address the effect of p25 generation on aberrant Cdk5 activation in the P301S mouse brain, we crossed P301S mice with Δp35KI mice, in which endogenous p35 is replaced with cleavage registrant mutant p35 incapable of p25 generation (Seo et al., 2014). As expected, p25 was undetected in P301S;Δp35KI mice hippocampal lysates (Figure 1A, B). The expression of mutant Δp35 protein tagged with triple HA was confirmed by immunoblotting with an anti-HA antibody (Figure 1A). We then examined Cdk5 activity in these mice and found that inhibition of p25 generation normalized Cdk5 activity in P301S mice to the levels of WT (Figure 1C). These data indicate that hyperactivation of Cdk5 in P301S mouse brains is mediated by abnormal p25 generation.

Blockade of p25 generation attenuates tauopathy in P301S mice brain.

Overexpression of human P301S mutant tau was shown to induce tau pathology including hyperphosphorylation of tau, increased levels of insoluble tau and the formation of neurofibrillary tangles (Yoshiyama et al., 2007). Although, the precise mechanisms of mutant-driven tau hyperphosphorylation remains unclear, a conformational change induced by such mutations is proposed to trigger phosphorylation of other residues of tau by various kinases such as Cdk5 or GSK-3β, or inhibit dephosphorylation mediated by phosphatases (Mazanetz and Fischer, 2007; Kolarova et al., 2012). To address the contribution of p25/Cdk5 to tau hyperphosphorylation in P301S mouse brains, we performed immunohistochemistry with hippocampal slices from P301S mice, P301S;Δp35KI mice and their WT littermates. We observed significant reduction of pTau levels in the hippocampus from P301S;Δp35KI mice compared to those from P301S mice. (Figure 2A). With antibodies against two different pTau epitopes (pTau T181 and pTau S202), we performed western blotting and consistent with our immunostaining data, levels of pTau in hippocampal lysates from P301S;Δp35KI mice were significantly reduced compared to those of P301S mice, without changes in total levels of tau (Figure 2B, p=0.0097 for pTau T181, p=0.0396 for pTau S202, p=0.283 for Tau5).

Recent studies suggest that pathogenic tau seeds can spread across the brain and trigger tauopathy in regions it spreads toward (Clavaguera et al., 2009; Frost et al., 2009; de Calignon et al., 2012). Thus, we asked whether a reduction of phosphorylated tau by p25/Cdk5 inhibition affects tau seeding activity in P301S

412 mouse brains. To measure tau seeding activity, we employed a FRET-based flow
413 cytometry biosensor assay reported recently (Holmes et al., 2014). This study
414 showed that tau seeding activity of lysates from P301S mice could be detected as
415 early as 2 months of age. Therefore, we prepared biosensor HEK293T cells
416 (expressing P301S mutant tau fused to either CFP or YFP) and treated them with
417 brain lysates from 2-month-old P301S, P301S;Δp35KI or WT littermate mice. After
418 24h, we measured FRET signals corresponding to the formation of tau aggregates
419 and found that while tau seeding remained significantly elevated relative to WT
420 brain lysates, inhibition of p25 production significantly reduced the seeding activity
421 of P301S brain lysates (Figure 2C, $p<0.0001$ by ANOVA). Altogether, these data
422 suggest that aberrant Cdk5 activity by p25 generation elevates tau
423 hyperphosphorylation and increases tau seeding activity in P301S mouse brain.
424
425 Inhibition of p25 restores synaptic function at mossy fiber-CA3 synapses in P301S
426 mice.
427 Hyperphosphorylation and aggregation of tau is associated with synapse loss
428 and cognitive impairment, and a significant reduction of synaptic density was
429 observed in the hippocampal CA3 region of P301S mice by 3 months of age
430 (Yoshiyama et al., 2007). To address the effect of p25/Cdk5 inhibition on tauopathy-
431 mediated synaptic loss, we measured synaptic density using an anti-synaptophysin
432 antibody in the CA3 region of 4-month-old P301S, P301S;Δp35KI and WT littermate
433 mice. Consistent with previous observations, P301S mice showed significantly
434 reduced levels of synaptophysin in CA3 compared to their WT littermates (Figure

435 3A). We also observed a trend toward to a reduction of synaptophysin levels in CA1
436 of P301S mice compared to WT, although it was not statistically significant (data not
437 shown). This synaptic loss in CA3 was completely reversed to the levels of WT by
438 inhibiting p25 generation (Figure 3A, p=0.0005 by ANOVA). To functionally analyze
439 synapse integrity, we next performed extracellular field recordings to measure
440 synaptic strength and long-term potentiation (LTP) at mossy fiber-CA3 synapses.
441 We observed that while basal synaptic transmission in P301S mice was reduced
442 compared to WT controls, inhibition of p25 in P301S mice significantly rescued this
443 effect. Importantly, neither Δp35KI mice or P301S;Δp35KI mice exhibited different
444 basal synaptic transmission compared to controls. The reduced baseline
445 transmission in P301S mice seems to be due to a reduction of synapse number
446 rather than an alteration of presynaptic neurotransmitter release because paired-
447 pulse facilitation ratios were not different between P301S and WT mice (Figure 3B).
448 Consistent with the loss of synaptic density, P301S mice did not show any
449 potentiation of field excitatory postsynaptic potentials (fEPSP) after three high-
450 frequency stimulations. However, similar to control and Δp35KI mice,
451 P301S;Δp35KI mice showed about 150% potentiation of fEPSP by the stimulations
452 (Figure 3C, p=0.0013 by ANOVA), indicating the restoration of synaptic plasticity by
453 p25 inhibition in P301S mice.
454
455 Inhibition of p25 generation reduces the levels of pTau in human cerebral organoids
456 carrying a P301L mutation in tau.

To validate the effect of p25 generation on tau hyperphosphorylation in human model systems, we utilized iPSCs derived from fibroblasts from a FTD patient carrying the Tau P301L mutation (*Silva, Watson, Tsai, Haggarty et al. Manuscript in preparation*). We then derived 3D human cerebral organoids from this iPSC line (MGH-2046) as well as from the non-mutant control line (MGH-2069) as reported previously (Raja et al., 2016). This system enabled us to address the role of p25 in tau hyperphosphorylation in the context of a tau mutation associated with different forms of tauopathy, as both tau and p35 are highly expressed in neurons. Two-month old organoids derived from iPSCs carrying the P301L mutation showed higher p25/p35 protein ratios compared to those derived from the non-mutant control (Figure 4A, p=0.038). To determine the role of p25/Cdk5 in tau hyperphosphorylation, we generated isogenic lines in which endogenous p35 is replaced with Δp35 protein by targeting Cas9 to the endogenous *CDK5R1* locus (encoding p35) alongside a template donor oligonucleotide harboring the Δp35 DNA sequence (Figure 4B). Sanger sequencing confirmed the incorporation of Δp35 sequence into the genome (Figure 4C). Top three of potential off-target sites predicted using CRISPR design tool (crispr.mit.edu) were inspected and sequencing data showed that no off-target effect was present in these regions (data not shown). Two-month old organoids from P301L iPSCs and P301L;Δp35KI isogenic lines were subjected to western blotting experiments. We first measured the levels of p25 generation in both groups and observed a significant reduction of p25 abundance by this genetic manipulation in human cerebral organoids. (Figure 4D, p=0.0092). We then examined the levels of pTau using two different antibodies (pTau S202 and

pTau T181) as well as total tau. Consistent with the data from our mouse study, we observed a substantial reduction of pTau levels in P301L;Δp35KI organoids compared to P301L organoids (Figure 4D, p=0.002 for pTau S202, p<0.0001 for pTau T181). We also observed a similar reduction in total tau levels (p=0.0029). And there was a trend to pTau/total tau being reduced, although it was not statistically significant. These effects on total tau do not appear to result from a reduced number of neurons, as indicated by comparable levels of NeuN (p=0.94), and could instead be due to the reduced aggregation of unphosphorylated vs. phosphorylated tau. The expression of synaptophysin was higher in P301L;Δp35KI organoids, which is also consistent with the observation from Δp35KI mice (Figure 4D, p=0.0287). Immunofluorescence analysis of the cerebral organoids also confirmed a reduction of pTau levels in P301L organoids by inhibition of p25 (Figure 4E, p=0.023). These data provide the first demonstration in a human neuronal culture system that disruption of p25/CDK5 activity can ameliorate tauopathy phenotypes.

Discussion

While the relationship between p25/Cdk5 and amyloid pathology has been an active area of interest, the impact of p25 inhibition upon another hallmark of AD, tauopathy, is less clear. Cdk5 hyperactivation by overexpressing p25 was shown to induce tauopathy in mouse brains (Cruz et al., 2003; Noble et al., 2003). However, the contribution of p25/Cdk5 complex to the development of tauopathy under pathological conditions by loss-of-function study has not been investigated. In this study, by genetically abolishing p25 generation, we have attempted to address whether p25 generation is necessary for aspects of tau-associated pathologies.

In the brain of P301S mice, a model of FTD, we found that p25/Cdk5 inhibition significantly reduces hyperphosphorylation of tau and its seeding activity. The levels of pTau and tau seeding activity in P301S;Δp35KI mice are still higher than those of WT mice because these mice significantly overexpress P301S tau. However, we found that inhibition of p25 generation is sufficient to restore synaptic integrity and function in this animal. To further determine the role of p25/Cdk5 in mutant tau-mediated pathology in human neurons, we turned to iPSC systems. Previous studies showed that human neurons differentiated from iPSCs of FTD patients carrying mutations in tau expressed higher levels of pTau and total tau compared to those from unaffected individuals (Fong et al., 2013; Silva et al., 2016). This effect does not appear to be due to increased number of neurons by early maturation because the levels of neuronal markers were not affected. These data showed that pathogenic

526 mutant tau induced hyperphosphorylation of tau as well as accumulation of total
527 tau, which could be caused by abnormal protein folding and impaired clearance of
528 this pathogenic protein. Using the CRISPR/Cas9 genome editing technique, we have
529 created isogenic lines of human iPSCs derived from a FTD patient carrying a P301L
530 mutation in the *MAPT* gene, with endogenous p35 replaced with Δp35. Cerebral
531 organoids derived from these isogenic iPSC lines demonstrated that blockade of p25
532 production reduced tau phosphorylation on multiple epitopes as well as lowering
533 total tau. As noted above, the effect on total tau levels could be due to enhanced
534 clearance of unphosphorylated tau. It is important to note that we didn't observe
535 such a reduction of total tau in P301S;Δp35KI mice compared to P301S mice. This
536 discrepancy could be from characteristics of two different model systems. Unlike
537 cerebral organoids that express endogenous levels of mutant tau, P301S mice
538 overexpresses mutant tau at levels more than five-fold higher than endogenous tau.
539 This could lower the efficiency to reduce expression of total tau even though p25
540 inhibition attenuates hyperphosphorylation of tau.
541
542 Interestingly, we observed that inhibition of p25 generation increases levels of
543 synaptophysin in both the P301S mice brain and Tau P301L organoids. Tau is
544 generally localized to the axons of neurons, however, hyperphosphorylated tau
545 accumulates in the somatodendritic compartment. This leads to mislocalization of
546 tau-interacting proteins such as the Fyn kinase. Previously, it was shown that
547 abnormal expression of Fyn followed by tau mislocalization at the synapse results in
548 the phosphorylation and activation of NMDA receptors, leading to neurotoxicity

549 (Ittner et al., 2010). We showed previously that NMDA receptor activation leads to
550 p25 generation, which subsequently causes synaptic depression (Seo et al., 2014).
551 Therefore, it is conceivable that p25 generation not only facilitates tau
552 hyperphosphorylation by leading to aberrant Cdk5 activation, but also mediates
553 neurotoxicity-induced synaptic depression and subsequent synaptic loss at the
554 synapses of brains with tauopathy.
555
556 In the progression of AD, an increase of Aβ is apparent as much as a couple of
557 decades before the onset of clinical symptoms (Jack et al., 2010). Aβ accumulation is
558 followed by hyperphosphorylation of tau, subsequent neuronal loss and cognitive
559 impairment. Although this suggests that Aβ could cause abnormal phosphorylation
560 of tau, the lack of tauopathy in mouse models of amyloidosis is perplexing. One
561 potential explanation is the different nature of the tau species in mouse versus
562 humans. Mouse does not express certain tau isoforms, thus it cannot recapitulate
563 the human four-repeat tau (4R-tau):three-repeat tau (3R-tau) ratio, changes in
564 which have been associated with the formation of tauopathy (Adams et al., 2010;
565 Schoch et al., 2016). Recent studies using iPSCs-derived neurons from AD patients
566 showed that this human model system nicely recapitulates both upregulation of Aβ
567 and hyperphosphorylation of tau (Israel et al., 2012; Muratore et al., 2014).Cdk5 is a
568 well-established tau kinase. Because we saw the beneficial effect of p25/Cdk5
569 inhibition on Aβ-induced pathology in the 5XFAD mouse model (Seo et al., 2014)
570 and on tauopathy in human model systems, we speculate that p25/Cdk5 mediates
571 Aβ-induced hyperphosphorylation of tau. And this further increases p25 generation

572 and Cdk5 hyperactivation as forming a feed-forward loop. p25/Cdk5 could also
573 facilitate tau phosphorylation by other kinases such as GSK-3β (Kimura et al., 2014).
574 As such, inhibition of p25/Cdk5 would likely be beneficial in this system.
575
576 In conclusion, our study using P301S;Δp35KI mice and P301L;Δp35KI iPSCs
577 suggest that inhibition of p25/Cdk5 is effective in ameliorating disease-causing
578 mutant tau-mediated pathology. Therefore, further efforts to develop inhibitors of
579 p25-mediated Cdk5 dysregulation are warranted and could benefit both AD and
580 FTD patients.
581
582
583
584
585
586
587
588
589
590
591
592
593
594

595 **References**

596

597 Adams SJ, DeTure MA, McBride M, Dickson DW, Petrucelli L (2010) Three repeat
598 isoforms of tau inhibit assembly of four repeat tau filaments. PLoS ONE
599 5:e10810.

600 Ahlijanian MK, Barrezueta NX, Williams RD, Jakowski A, Kowsz KP, McCarthy S,
601 Coskran T, Carlo A, Seymour PA, Burkhardt JE, Nelson RB, McNeish JD (2000)
602 Hyperphosphorylated tau and neurofilament and cytoskeletal disruptions in
603 mice overexpressing human p25, an activator of cdk5. Proc Natl Acad Sci USA
604 97:2910–2915.

605 Clavaguera F, Bolmont T, Crowther RA, Abramowski D, Frank S, Probst A, Fraser G,
606 Stalder AK, Beibel M, Staufenbiel M, Jucker M, Goedert M, Tolnay M (2009)
607 Transmission and spreading of tauopathy in transgenic mouse brain. Nat Cell
608 Biol 11:909–913.

609 Cruz JC, Tseng H-C, Goldman JA, Shih H, Tsai L-H (2003) Aberrant Cdk5 activation by
610 p25 triggers pathological events leading to neurodegeneration and
611 neurofibrillary tangles. Neuron 40:471–483.

612 de Calignon A, Polydoro M, Suárez-Calvet M, William C, Adamowicz DH, Kopeikina
613 KJ, Pitstick R, Sahara N, Ashe KH, Carlson GA, Spires-Jones TL, Hyman BT (2012)
614 Propagation of tau pathology in a model of early Alzheimer's disease. Neuron
615 73:685–697.

616 Fong H, Wang C, Knoferle J, Walker D, Balestra ME, Tong LM, Leung L, Ring KL,
617 Seeley WW, Karydas A, Kshirsagar MA, Boxer AL, Kosik KS, Miller BL, Huang Y
618 (2013) Genetic correction of tauopathy phenotypes in neurons derived from
619 human induced pluripotent stem cells. Stem Cell Reports 1:226–234.

620 Frost B, Jacks RL, Diamond MI (2009) Propagation of tau misfolding from the
621 outside to the inside of a cell. J Biol Chem 284:12845–12852.

622 Hashiguchi M, Saito T, Hisanaga S-I, Hashiguchi T (2002) Truncation of CDK5
623 activator p35 induces intensive phosphorylation of Ser202/Thr205 of human
624 tau. J Biol Chem 277:44525–44530.

625 Holmes BB, Furman JL, Mahan TE, Yamasaki TR, Mirbaha H, Eades WC, Belaygorod
626 L, Cairns NJ, Holtzman DM, Diamond MI (2014) Proteopathic tau seeding
627 predicts tauopathy in vivo. PNAS 111:E4376–E4385.

628 Israel MA, Yuan SH, Bardy C, Reyna SM, Mu Y, Herrera C, Hefferan MP, Van Gorp S,
629 Nazor KL, Boscolo FS, Carson CT, Laurent LC, Marsala M, Gage FH, Remes AM,
630 Koo EH, Goldstein LSB (2012) Probing sporadic and familial Alzheimer's disease
631 using induced pluripotent stem cells. Nature 482:216–220.

632 Ittner LM, Ke YD, Delerue F, Bi M, Gladbach A, van Eersel J, Wölfing H, Chieng BC,
633 Christie MJ, Napier IA, Eckert A, Staufenbiel M, Hardeman E, Götz J (2010)
634 Dendritic function of tau mediates amyloid-beta toxicity in Alzheimer's disease
635 mouse models. Cell 142:387–397.

636 Jack CR, Knopman DS, Jagust WJ, Shaw LM, Aisen PS, Weiner MW, Petersen RC,
637 Trojanowski JQ (2010) Hypothetical model of dynamic biomarkers of the
638 Alzheimer's pathological cascade. Lancet Neurol 9:119–128.

639 Kimura T, Ishiguro K, Hisanaga S-I (2014) Physiological and pathological
640 phosphorylation of tau by Cdk5. Front Mol Neurosci 7:65.

641 Kolarova M, García-Sierra F, Bartos A, Ricny J, Ripova D (2012) Structure and
642 pathology of tau protein in Alzheimer disease. Int J Alzheimers Dis
643 2012:731526.

644 Komor AC, Badran AH, Liu DR (2017) CRISPR-Based Technologies for the
645 Manipulation of Eukaryotic Genomes. Cell 168:20–36.

646 Kondadi AK, Wang S, Montagner S, Kladt N, Korwitz A, Martinelli P, Herholz D, Baker
647 MJ, Schauss AC, Langer T, Rugarli EI (2014) Loss of the m-AAA protease subunit
648 AFG_3L_2 causes mitochondrial transport defects and tau hyperphosphorylation.
649 EMBO J 33:1011–1026.

650 Kusakawa G, Saito T, Onuki R, Ishiguro K, Kishimoto T, Hisanaga S (2000) Calpain-
651 dependent proteolytic cleavage of the p35 cyclin-dependent kinase 5 activator
652 to p25. J Biol Chem 275:17166–17172.

653 Lee MS, Kwon YT, Li M, Peng J, Friedlander RM, Tsai LH (2000) Neurotoxicity
654 induces cleavage of p35 to p25 by calpain. Nature 405:360–364.

655 Mazanetz MP, Fischer PM (2007) Untangling tau hyperphosphorylation in drug

design for neurodegenerative diseases. Nat Rev Drug Discov 6:464–479.

Miller N, Feng Z, Edens BM, Yang B, Shi H, Sze CC, Hong BT, Su SC, Cantu JA, Topczewski J, Crawford TO, Ko C-P, Sumner CJ, Ma L, Ma Y-C (2015) Non-aggregating tau phosphorylation by cyclin-dependent kinase 5 contributes to motor neuron degeneration in spinal muscular atrophy. J Neurosci 35:6038–6050.

Mou X, Wu Y, Cao H, Meng Q, Wang Q, Sun C, Hu S, Ma Y, Zhang H (2012) Generation of disease-specific induced pluripotent stem cells from patients with different karyotypes of Down syndrome. Stem Cell Res Ther 3:14.

Muratore CR, Rice HC, Srikanth P, Callahan DG, Shin T, Benjamin LNP, Walsh DM, Selkoe DJ, Young-Pearse TL (2014) The familial Alzheimer's disease APPV717I mutation alters APP processing and Tau expression in iPSC-derived neurons. Hum Mol Genet 23:3523–3536.

Nath R, Davis M, Probert AW, Kupina NC, Ren X, Schielke GP, Wang KK (2000) Processing of cdk5 activator p35 to its truncated form (p25) by calpain in acutely injured neuronal cells. Biochem Biophys Res Commun 274:16–21.

Noble W, Olm V, Takata K, Casey E, Mary O, Meyerson J, Gaynor K, LaFrancois J, Wang L, Kondo T, Davies P, Burns M, Veeranna, Nixon R, Dickson D, Matsuoka Y, Ahlijanian M, Lau L-F, Duff K (2003) Cdk5 is a key factor in tau aggregation and tangle formation in vivo. Neuron 38:555–565.

676 Patrick GN, Zukerberg L, Nikolic M, la Monte de S, Dikkes P, Tsai LH (1999)
677 Conversion of p35 to p25 deregulates Cdk5 activity and promotes
678 neurodegeneration. Nature 402:615–622.

679 Piedrahita D, Hernández I, López-Tobón A, Fedorov D, Obara B, Manjunath BS,
680 Boudreau RL, Davidson B, Laferla F, Gallego-Gómez JC, Kosik KS, Cardona-
681 Gómez GP (2010) Silencing of CDK5 reduces neurofibrillary tangles in
682 transgenic alzheimer's mice. J Neurosci 30:13966–13976.

683 Raja WK, Mungenast AE, Lin Y-T, Ko T, Abdurrob F, Seo J, Tsai L-H (2016) Self-
684 Organizing 3D Human Neural Tissue Derived from Induced Pluripotent Stem
685 Cells Recapitulate Alzheimer's Disease Phenotypes. PLoS ONE 11:e0161969.

686 Ran FA, Hsu PD, Wright J, Agarwala V, Scott DA, Zhang F (2013) Genome engineering
687 using the CRISPR-Cas9 system. Nat Protoc 8:2281–2308.

688 Schoch KM, DeVos SL, Miller RL, Chun SJ, Norrbom M, Wozniak DF, Dawson HN,
689 Bennett CF, Rigo F, Miller TM (2016) Increased 4R-Tau Induces Pathological
690 Changes in a Human-Tau Mouse Model. Neuron 90:941–947.

691 Seo J, Giusti-Rodríguez P, Zhou Y, Rudenko A, Cho S, Ota KT, Park C, Patzke H,
692 Madabhushi R, Pan L, Mungenast AE, Guan J-S, Delalle I, Tsai L-H (2014)
693 Activity-dependent p25 generation regulates synaptic plasticity and Aβ-induced
694 cognitive impairment. Cell 157:486–498.

695 Siegert S, Seo J, Kwon EJ, Rudenko A, Cho S, Wang W, Flood Z, Martorell AJ, Ericsson

696 M, Mungenast AE, Tsai L-H (2015) The schizophrenia risk gene product miR-137
697 alters presynaptic plasticity. Nat Neurosci 18:1008–1016.

698 Silva MC, Cheng C, Mair W, Almeida S, Fong H, Biswas MHU, Zhang Z, Huang Y,
699 Temple S, Coppola G, Geschwind DH, Karydas A, Miller BL, Kosik KS, Gao F-B,
700 Steen JA, Haggarty SJ (2016) Human iPSC-Derived Neuronal Model of Tau-
701 A152T Frontotemporal Dementia Reveals Tau-Mediated Mechanisms of
702 Neuronal Vulnerability. Stem Cell Reports 7:325–340.

703 Van den Haute C, Spittaels K, Van Dorpe J, Lasrado R, Vandezande K, Laenen I, Geerts
704 H, Van Leuven F (2001) Coexpression of human cdk5 and its activator p35 with
705 human protein tau in neurons in brain of triple transgenic mice. Neurobiol Dis
706 8:32–44.

707 Yoshiyama Y, Higuchi M, Zhang B, Huang S-M, Iwata N, Saido TC, Maeda J, Suhara T,
708 Trojanowski JQ, Lee VM-Y (2007) Synapse loss and microglial activation precede
709 tangles in a P301S tauopathy mouse model. Neuron 53:337–351.

710 Zhang X, Hernández I, Rei D, Mair W, Laha JK, Cornwell ME, Cuny GD, Tsai L-H, Steen
711 JAJ, Kosik KS (2013a) Diaminothiazoles modify Tau phosphorylation and
712 improve the tauopathy in mouse models. J Biol Chem 288:22042–22056.

713 Zhang Z, Almeida S, Lu Y, Nishimura AL, Peng L, Sun D, Wu B, Karydas AM, Tartaglia
714 MC, Fong JC, Miller BL, Farese RV, Moore MJ, Shaw CE, Gao F-B (2013b)
715 Downregulation of microRNA-9 in iPSC-derived neurons of FTD/ALS patients
716 with TDP-43 mutations. PLoS ONE 8:e76055.

Figure Legends

Figure 1. Inhibition of p25 generation abolishes Cdk5 hyperactivation in P301S mice brain.

(A) Levels of p25 in WT, P301S and P301S;Δp35KI hippocampus. Δp35 expression in P301S;Δp35KI was confirmed by immunoblotting with an anti-HA antibody. The asterisk represents a nonspecific background band.

(B) The bar graph represents relative immunoreactivity of p25/p35 compared to WT (Student's t test).

(C) IP-linked Cdk5 kinase assays were performed on WT, P301S and P301S;Δp35KI hippocampal lysates (n=3~5 per group; p=0.0009 by ANOVA).

*p<0.05, **p<0.01, ***p<0.001 by Student's t test or Tukey's post hoc analysis; error bars ±SEM.

Figure 2. Inhibition of p25/Cdk5 attenuates hyperphosphorylation of tau and its seeding activity in P301S mice brain.

(A) Immunohistochemistry with an anti-pTau T181 antibody in hippocampal CA1 of WT, P301s and P301S;Δp35KI mice. Scale bar, 20 μm.

(B) Relative levels of pTau T181, pTau S202 and total tau in P301S and P301S;Δp35KI hippocampus normalized to P301S. (n=4~8, per group; Student's t test).

(C) Cortical lysates from 2-month-old WT, P301s and P301S;Δp35KI mice were added to biosensor HEK293T cells and their tau seeding activity were quantified by measuring FRET signals. (n=4 per group; p<0.0001 by ANOVA).

*p<0.05, **p<0.01, ***p<0.001 by Student's t test or Tukey's post hoc analysis; error bars ±SEM.

Figure 3. Blockade of p25 generation restores synaptic integrity and function in hippocampal CA3 region of P301S mice.

(A) Immunohistochemistry with an anti-synaptophysin antibody in hippocampal CA3 of WT, P301s and P301S;Δp35KI mice. Right: the bar graphs represent the relative immunoreactivity of synaptophysin in WT, P301S and P301S;Δp35KI normalized to WT. (n=3~5 per group; p=0.0005 by ANOVA). Scale bar, 20 μm.

(B) Left: input-output curves from the fEPSP amplitude against the fiber volley amplitude at a range of stimulus intensities. Right: paired-pulse facilitation (fEPSP2 / fEPSP1) was measured at various interstimulus intervals.

(C) LTP was induced by 3x HFS at mossy fiber-CA3 synapses. Sample traces represent fEPSPs at 1 min before (gray) and 1 hr after (block) HFS. Scale bars, 0.5 mV and 10 ms. Right: the magnitude of LTP was calculated by comparing the average slopes of fEPSPs during the last 5 min of recordings with those recorded before stimulation. (n=4~6 per group; p=0.0013 by ANOVA)

*p<0.05, **p<0.01, ***p<0.001 by Student's t test or Tukey's post hoc analysis; error bars ±SEM.

Figure 4. p-Tau levels in organoids derived from a FTD patient iPSCs are reduced by inhibition of p25 expression.

(A) Relative levels of p35 and p25 in organoids derived from non-mutant control (MGH 2069) or Tau P301L (MGH 2046) iPSCs. (n=3 biological replicates, 3~4 organoids were pooled for each blot).

(B) Schematics of Δp35KI isogenic line generation from a FTD patient iPSCs carrying the Tau P301L mutation.

(C) Sanger sequencing confirms the insertion of a desired repair template into a FTD patient iPSCs.

(D) Relative levels of p35, p25, synaptophysin, NeuN, pTau T181, pTau S202 and total tau in organoids derived from P301L or P301L;Δp35KI iPSCs. Right: the bar graph represents the quantification of relative immunoreactivity for each protein in organoids normalized to P301L organoids. (n=4 biological replicates, 3~4 organoids were pooled for each blot).

(E) Immunohistochemistry with an anti-pTau T181 antibody in organoids derived from P301L or P301L;Δp35KI iPSCs. Scale bar, 5 μm. Right: the bar graph represents the relative immunoreactivity of pTau T181 in each group. (n=6 per group)

*p<0.05, **p<0.01, ***p<0.001 by Student's t test; error bars ±SEM.

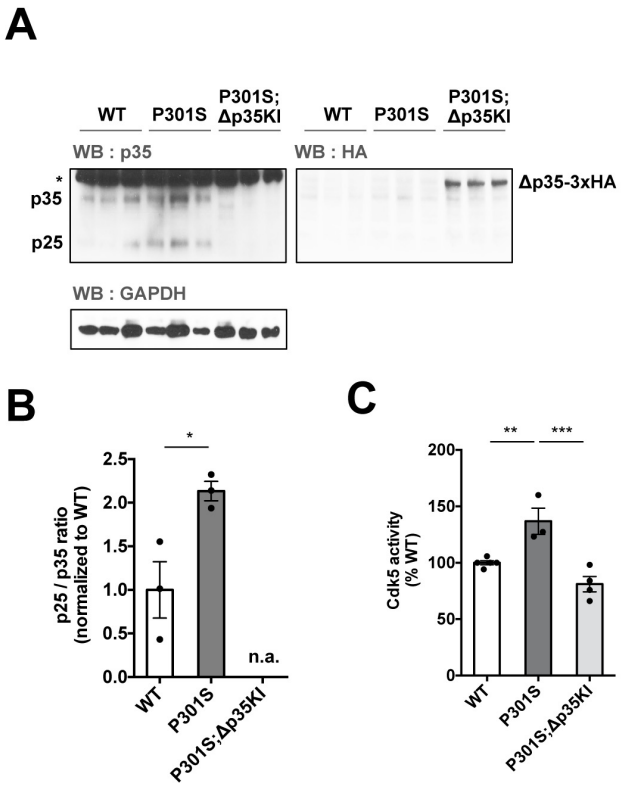

Figure 1

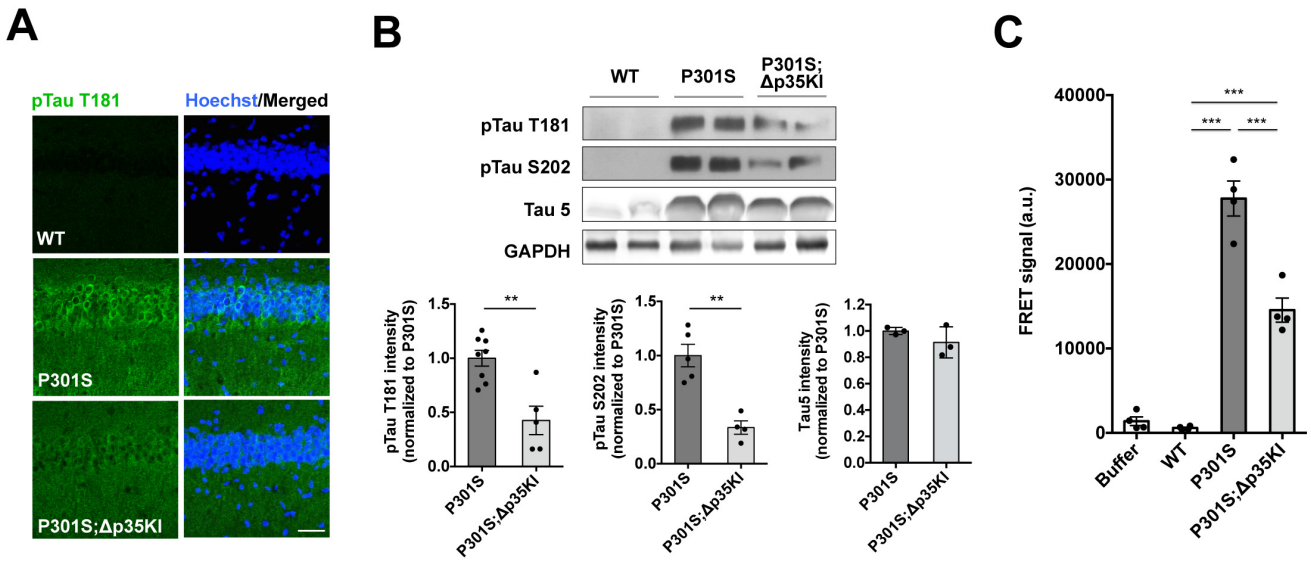

Figure 2

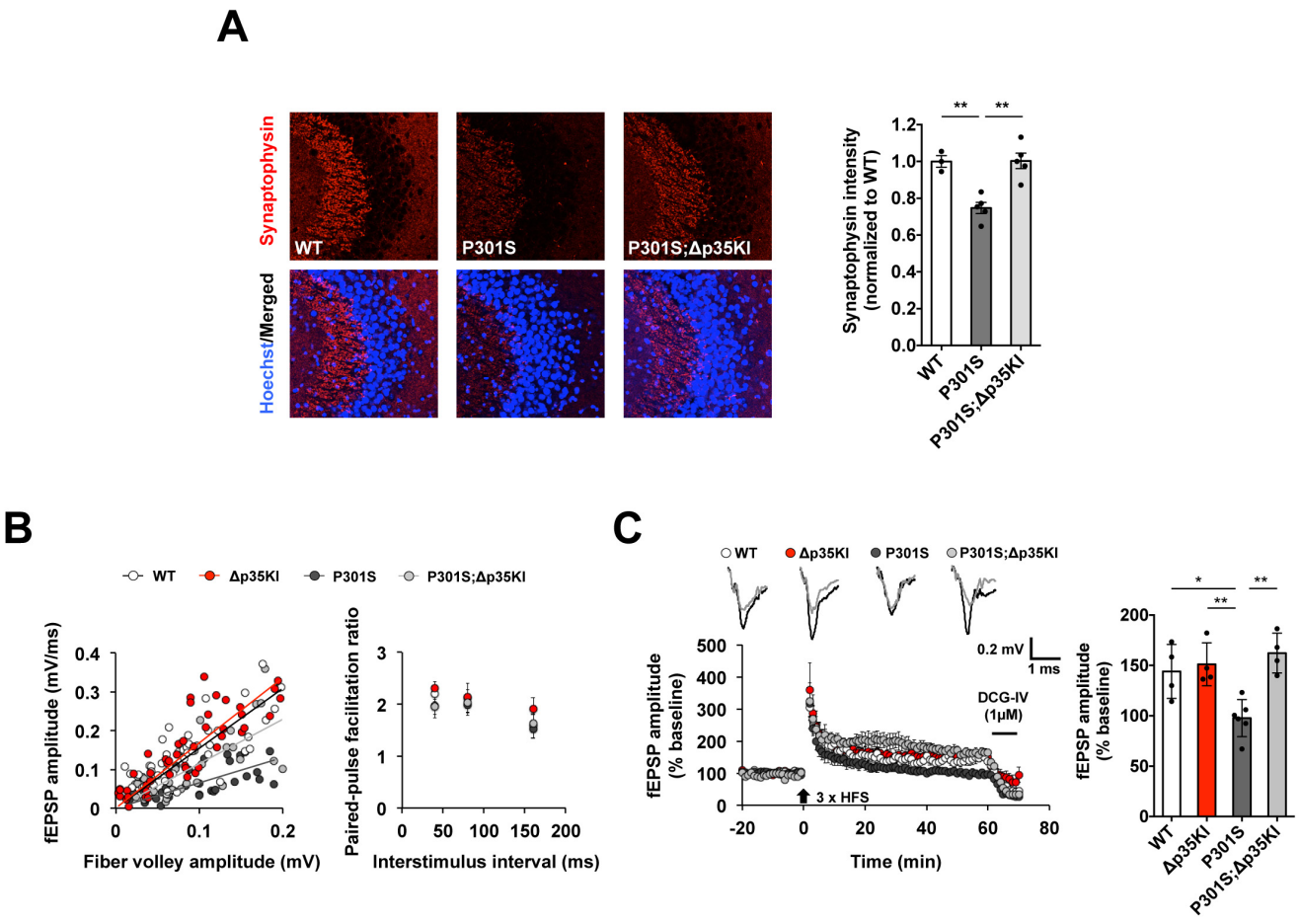

Figure 3

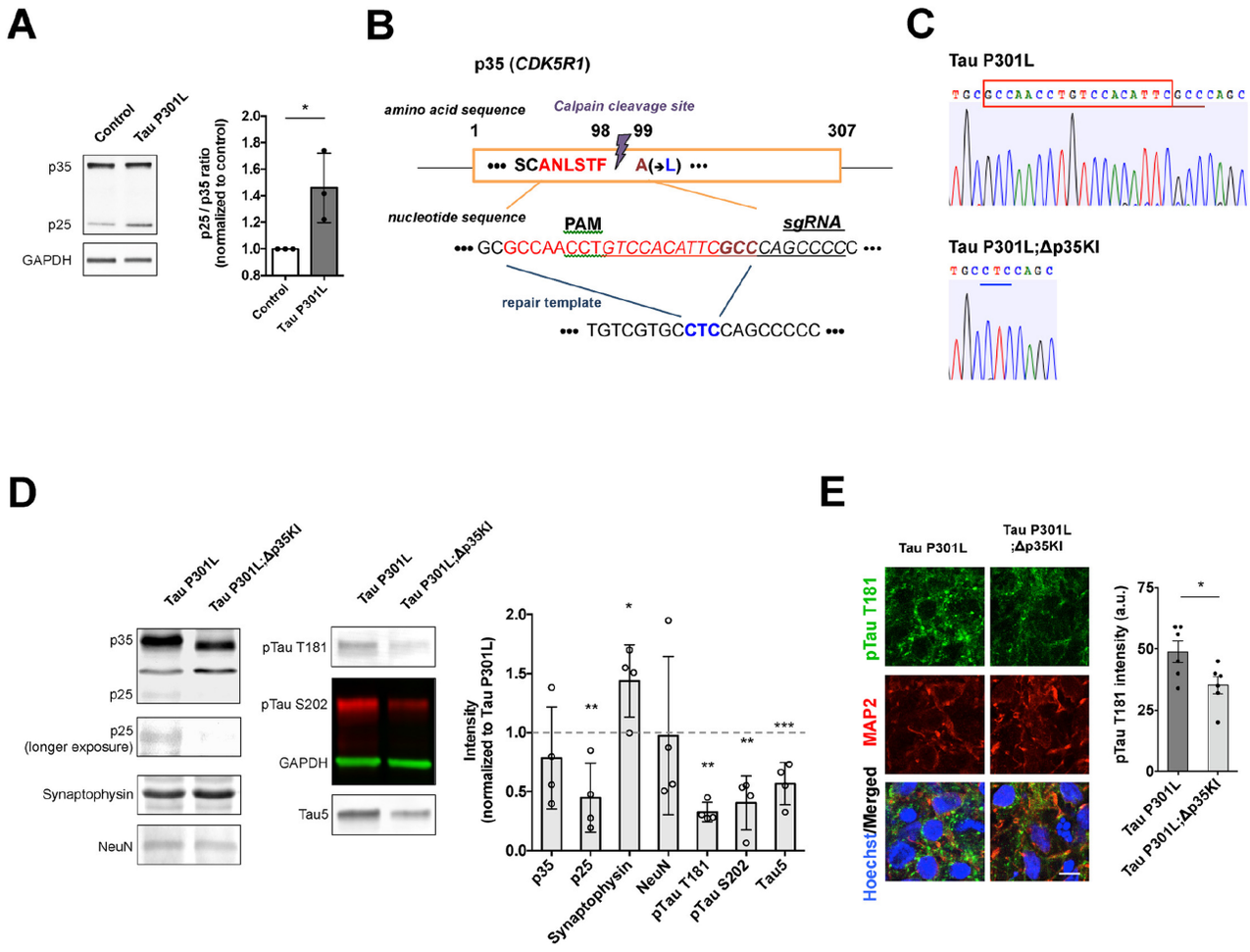

Figure 4